Anal. Chem. **2002,** *74,* 4027−4036

Rational Design of Potentiometric Trace Level Ion Sensors. A Ag^+-Selective Electrode with a 100 ppt Detection Limit

Alan Ceresa,[†] Aleksandar Radu,[‡] Shane Peper,[‡] Eric Bakker,*[,‡] and Ernő Pretsch*[,†]

Laboratorium für Organische Chemie, ETH Hönggerberg, CH-8093 Zürich, Switzerland, and Department of Chemistry, Auburn University, Auburn, Alabama 36849

Submicromolar to picomolar lower detection limits have recently been obtained with various polymer membrane ion-selective electrodes by minimizing biases due to ion fluxes through the membrane. For the best performance, the compositions of the membrane and inner solution should be optimized for each application. Given the number of parameters to be adjusted, it has been difficult to find the best parameters for a target sample. In this paper, a much simplified and more practical steady-state model of zero-current ion fluxes is derived, which is based on measurable parameters. The model allows one to predict achievable lower detection limits for a membrane with given selectivities. It can also be used to predict the optimal composition of the inner filling solution for the measurement of samples with a known, typical ionic background. Selectivity coefficients of monovalent and divalent analyte ions required for desired detection limits in drinking water are calculated. As an application of the proposed general recipe, a silver-selective electrode is developed on the basis of the ionophore *O,O″*-bis[2-(methylthio)ethyl]-*tert*-butylcalix[4]arene. With the predicted optimal composition of the inner electrolyte, its lower detection limit is found to be 10^{-9} M or 100 ppt Ag^+ with an ionic background of 10^{-5} M $LiNO_3$, which is very close to the expected value.

In trace level analysis, sufficiently low detection limits in the submicromolar range must be achieved in the presence of rather high activities (on the order of millimolar) of other species. For a long time, polymer membrane ion-selective electrodes (ISEs) were not considered to be adequate tools for trace ion analysis. Instead, they were perceived as chemical sensors of relatively low selectivity, and their lower detection limits, even in the absence of added ionic interferences, used to be in the micromolar range.[1−3] Their universally accepted application was mainly the detection of relatively high concentrations of selected ions in complex matrixes such as whole blood.[4] Only recently, it became clear that the lack of a low detection limit was not an inherent property of this type of sensor but a consequence of the commonly accepted experimental setup. Ion-selective membranes contain a rather high concentration of the primary ion−ionophore complex, usually on the order of 5 mM. With a membrane thickness of 200 μm and a radius of 3 mm, a typical ion-selective membrane contains 30 nmol of primary ions. If a mechanism exists that can expel just 1% of these ions into a surrounding 10-mL solution, these ions would concentrate the sample by 30 nM. In practice, the observed bias on the potentiometric measurement would be even larger, since ISE membranes are sensitive to concentration changes in the sample-phase boundary, not the sample bulk.

It is now known that the most important mechanism of primary ion release from the membrane to the surrounding solution is the counterdiffusion with interfering ions. Even the exchange of just a minute fraction of primary ions by interfering ions at the membrane surface gives rise to sufficient concentration polarizations within the membrane interior that lead to a continuous flux of primary ions into the sample. In dilute solutions, the resulting ion fluxes determine the sample concentration of the primary ion at the membrane phase boundary, for which the electrode is responsive. Traditionally, the backside of the sensing membrane is in contact with a rather concentrated solution (the so-called internal filling solution) of the analyte ion. However, even under zero-current conditions, ions are able to diffuse across the sensing membrane, by countertransport from the sample to the inner solution of another ion of the same charge sign or cotransport from the inner solution to the sample of an ion of opposite charge. These processes maintain a significantly high ion activity in the diffusion layer near the membrane even if the sample bulk virtually does not contain any analyte ion. Earlier, this minimum ion activity was erroneously assumed to be the inherent lower detection limit of these devices. Today, various experimental techniques are available to reduce or avoid this bias and to develop ISEs with improved detection limits.[5−7] So far, ISEs with improved lower detection limits for K^+, NH_4^+, Ca^{2+}, Pb^{2+}, and Cd^{2+} have been developed.[5,6,8−11]

[†] ETH Zürich.
[‡] Auburn University.

(1) Umezawa, Y. *Handbook of Ion-Selective Electrodes: Selectivity Coefficients*; CRC Press: Boca Raton, FL, 1990.
(2) Bühlmann, P.; Pretsch, E.; Bakker, E. *Chem. Rev.* **1998**, *98*, 1593.
(3) Bakker, E.; Bühlmann, P.; Pretsch, E. *Electroanalysis* **1999**, *11*, 915.
(4) Yim, H. S.; Kibbey, C. E.; Ma, S. C.; Kliza, D. M.; Liu, D.; Park, S. B.; Torre, C. E.; Meyerhoff, M. E. *Biosens. Bioelectron.* **1993**, *8*, 1.
(5) Bakker, E.; Pretsch, E. *Trends Anal. Chem.* **2001**, *20*, 11.
(6) Bakker, E.; Pretsch, E. *Anal. Chem.*, in press.
(7) Pergel, E.; Gyurcsányi, R. E.; Tóth, K.; Lindner, E. *Anal. Chem.* **2001**, *73*, 4249.

10.1021/ac025548y CCC: $22.00
Published on Web 06/25/2002

In addition to the achievable lower detection limits, the selectivities of polymer membrane electrodes were also perceived to be insufficient for trace level applications. Surprisingly, it turned out that most of the published selectivity data were too pessimistic and that the true values are often many orders of magnitude better than reported in the original papers. Selectivity determination relies on measurements under conditions where only one kind of ion (analyte or interfering ion) is potential determining.[12,13] However, as a consequence of the above-described zero-current fluxes, strongly discriminated interfering ions are not potential determining in the traditional setup and the best possible selectivity coefficients measurable under such conditions are on the order of 10^{-4}–10^{-5}. Today, it is well established that unbiased selectivity coefficients can be better than these limiting values by up to 10 orders of magnitude.[5] Thus, it has been demonstrated recently that Pb^{2+} can be determined in drinking water and other environmental samples[11] with a lower detection limit that is 10 times below the action limit set by the Environmental Protection Agency.[14]

In recent years, the theory of the underlying transport processes has been developed and used for improving the design of ISEs for trace analysis. Originally, the equations describing ion exchange, coextraction, and diffusion were solved iteratively.[15,16] Later, implicit equations were derived that describe the phase boundary potential as a function of the composition of the inner solution, the membrane, and the sample and parameters including the distribution coefficients of the various species.[17] Although these parameters are related to the experimentally accessible selectivity coefficients, the direct use of the latter was not straightforward so far. Moreover, the existing theory does not allow one to predict the required selectivity coefficient for a given application.

In this paper, a new theoretical model is presented that allows one to calculate the optimal composition of the inner solution of an ISE based on a given membrane and target application. In contrast to earlier descriptions,[15–17] the application of these explicit equations only requires knowledge of the membrane composition, the experimentally determined selectivity coefficients, the concentration of interfering ions, and the ratio of the diffusion coefficients of the analyte ion in both phases. As compared to the earlier treatments, this model yields much simpler, explicit relationships between the detection limit and membrane selectivity and the compositions of membrane and inner solution. It forms so far the most appropriate basis for a rational design of ISEs with optimized lower detection limits. For example, the selectivity coefficients required to reach a desired detection limit can be calculated, along with the optimal composition of the inner solution. The model is applied to the design of a Ag^+ ISE with a lower detection limit of 10^{-9} M (100 ppt) in the presence of 10^{-5} M $LiNO_3$.

EXPERIMENTAL SECTION

Reagents. Poly(vinyl chloride) (PVC), bis(2-ethylhexyl) sebacate (DOS), sodium tetrakis[3,5-bis(trifluoromethyl)phenyl]-borate (NaTFPB), the Ag^+ ionophore *O,O″*-bis[2-(methylthio)-ethyl]-*tert*-butylcalix[4]arene, the cation exchanger Dowex Monosphere C-350, and tetrahydrofuran (THF) were from Fluka AG (CH-8071 Buchs, Switzerland). Aqueous solutions were prepared with freshly deionized water (18.0 MΩ cm specific resistance) obtained with a NANOpure reagent-grade water system (Barnstead, CH-4009 Basel, Switzerland). HNO_3, $LiNO_3$, NaCl, and KCl were of Suprapur grade from Merck (Darmstadt, Germany). $AgNO_3$ was obtained as a 0.1 M standard solution from Fluka.

Membranes. The membrane contained 0.023 mol kg^{-1} (1.83 wt %) Ag^+ ionophore, 0.0057 mol kg^{-1} (0.51 wt %) NaTFPB, 32.55 wt % PVC, and 65.11 wt % DOS. A membrane of ~200 μm was obtained by casting a solution of 500 mg of the membrane components in 5 mL of freshly distilled THF into a Petri dish of 5.9-cm i.d.

Electrodes. A disk of 6-mm diameter was punched from the above ion-selective membrane and glued to a plasticized PVC tubing of 4-mm i.d. with a THF/PVC slurry. For preparing the inner filling solutions, 3 g of the ion-exchange resin in the sodium form was equilibrated overnight with 3 mL of water containing 2 × 10^{-3} M $NaNO_3$ and different concentrations of $AgNO_3$ (10^{-3} and 10^{-4} M for the ISEs A and B, respectively). The resin selectivity $K_{Na,Ag}$, i.e., the equilibrium constant of the reaction Na-resin + Ag(aq) = Na(aq) + Ag-resin, was determined by equilibrating 0.1 g of the dry resin, as the Na^+ form, with 50 mL of a 10^{-4} M Ag^+ solution overnight. The Ag^+ concentration at equilibrium (2 × 10^{-7} M) was measured with ISE A. The free Ag^+ concentrations calculated from the resin selectivity (K_{NaAg} = 4.8) and capacity (5.2 × 10^{-3} mequiv/g)[10] were 3.2 × 10^{-7} and 8.3 × 10^{-8} M for ISEs A and B, respectively. The percentages of Ag^+ relative to the sites' concentration at the inner membrane surface were determined from potentiometric selectivity coefficients (= $10^{-7.4}$ and $10^{-6.8}$) and the pH and Ag^+ and Na^+ concentrations in the inner solution. They were 99.95% and 98.99% for ISEs A and B, respectively. The inner solution was in contact with the reference solution (2 × 10^{-3} M $NaNO_3$, 10^{-4} M NaCl) through 2 × 10^{-3} M $NaNO_3$ as bridge electrolyte. All ISEs were conditioned in 10^{-4} M $AgNO_3$ for 24 h.

EMF Measurements. Measurements were performed with a 16-channel electrode monitor (Lawson Labs Inc., Malvern, PA 19355) in a flow-through cell described earlier[18] at a flow rate of 2 mL/min. To prevent the formation of gas bubbles in the channels that would introduce noise, the solutions were degassed with argon for ~30 min. The calibration curves were measured by subsequent dilution with solutions containing 10^{-5} M $LiNO_3$ as background electrolyte. The response times were less than 5 min for the concentration changes from 10^{-5} to 10^{-6} M. The measuring times were 30 min and 4 h for the 10^{-7} and 10^{-8} M solutions, respectively, and 2 h for the more dilute ones. Data were taken during the last minute of the time period when the

(8) Sokalski, T.; Ceresa, A.; Zwickl, T.; Pretsch, E. *J. Am. Chem. Soc.* **1997**, *119*, 11347.
(9) Sokalski, T.; Ceresa, A.; Fibbioli, M.; Zwickl, T.; Bakker, E.; Pretsch, E. *Anal. Chem.* **1999**, *71*, 1210.
(10) Qin, W.; Zwickl, T.; Pretsch, E. *Anal. Chem.* **2000**, *72*, 3236.
(11) Ceresa, A.; Bakker, E.; Günther, D.; Hattendorf, B.; Pretsch, E. *Anal. Chem.* **2001**, *73*, 343.
(12) Bakker, E.; Bühlmann, P.; Pretsch, E. *Chem. Rev.* **1997**, *97*, 3083.
(13) Bakker, E.; Pretsch, E.; Bühlmann, P. *Anal. Chem.* **2000**, *72*, 1127.
(14) Lead and Copper Rule Minor Revisions; Environmental Protection Agency, EPA 815-F-99-010, 1999.
(15) Sokalski, T.; Zwickl, T.; Bakker, E.; Pretsch, E. *Anal. Chem.* **1999**, *71*, 1204.
(16) Zwickl, T.; Sokalski, T.; Pretsch, E. *Electroanalysis* **1999**, *11*, 673.
(17) Morf, W. E.; Badertscher, M.; Zwickl, T.; de Rooij, N. F.; Pretsch, E. *J. Phys. Chem. B* **1999**, *103*, 11346.
(18) Ceresa, A.; Sokalski, T.; Pretsch, E. *J. Electroanal. Chem.* **2001**, *501*, 70.

drifts were ≤±1 mV/h. Larger drifts of ∼−3 mV/h were observed after 4 h with the 10^{-8} M solution. To ensure that the $E°$ of the ISE cell assembly did not change during the measurement (∼10 h), the emf was recorded again in the starting solution at the end of each cycle. The ion activities were calculated according to the Debye−Hückel formalism.[19]

THEORY

Earlier treatments describing the ion flux-induced detection limit of polymer membrane ISEs were based on fundamental thermodynamic and kinetic parameters, i.e., ion-exchange and coextraction constants, stability constants, and diffusion coefficients.[15−17] This approach made it quite difficult to obtain compact results that would be valid for a number of cases and that could be directly correlated with experimental data. The treatment presented here is a dramatic simplification of those earlier descriptions. It incorporates the recently established selectivity theory, which was in turn based on thermodynamic equilibria at the sample−membrane interface. The steady-state zero-current ion flux processes can now be described on the basis of membrane selectivity, with the help of experimentally assessable selectivity coefficients. The equations derived here can be directly used to predict the achievable detection limits and to calculate the optimal composition of the inner solution.

The response of potentiometric sensors in the presence of any number of ions can be fully described by the phase boundary potential model.[20−23] For ions of the same charge, this model results in the Nicolsky−Eisenman equation (eq 1), where E_M is

$$E_M = E_I^0 + \frac{RT}{z_I F} \ln(a_I + \sum K_{IJ}^{pot} a_J^{z_I/z_J}) \quad (1)$$

the observed membrane potential, R, T, and F are the gas constant, the absolute temperature and the Faraday constant, respectively, a_I and a_J are the activities of the primary and interfering ions I (with charge z_I) and J (with charge z_J), K_{IJ}^{pot} is the potentiometric selectivity coefficient, and E_I^0 includes all constant potential contributions. Since this equation is not exact for $z_I \neq z_J$, more complex formalisms are required if a_I and $\sum K_{IJ}^{pot} a_J^{z_I/z_J}$ are comparable. For monovalent and divalent ions, the following eq 2 has

$$E_M = E_I^0 + \frac{RT}{z_I F} \ln\left[\frac{1}{2}\sum_{m1} K_{I,m1}^{pot\ 1/z_I} a_{m1} + \sqrt{\left(\frac{1}{2}\sum_{m1} K_{I,m1}^{pot\ 1/z_I} a_{m1}\right)^2 + \sum_{m2} K_{I,m2}^{pot\ 2/z_I} a_{m2}}\right]^{z_I} \quad (2)$$

been established to describe the corresponding mixed-ion response of ISEs:[23,24]

The summations in eq 2 are each performed for all monovalent (m1) and divalent (m2) sample ions. The monovalent or divalent primary ion is included in this summation with $K_{IJ}^{pot} = 1$.

For two ions I and J with different charges, eqs 1 and 2 lead to identical results as long as one of the ions is potential determining, i.e., for $a_I \gg K a_J^{z_I/z_J}$ and $a_I \ll K a_J^{z_I/z_J}$. The first limiting case is simply the Nernst equation for the primary ion I:

$$E_M = E_I^0 + \frac{RT}{z_I F} \ln a_I \quad (3)$$

and for the second limiting case (Nernst equation for the interfering ion) the emf does no longer depend on a_I. The lower detection limit has been defined as the cross section of the lines corresponding to these limiting cases as[25]

$$c_I(DL) = K_{IJ}^{pot} c_J^{z_I/z_J} \quad (4)$$

For simplicity, concentrations are used instead of activities in eq 4 and in the following. It is known that eq 4 generally predicts detection limits too low for highly selective ISEs, where ion fluxes are relevant.[5] A more appropriate description must therefore consider concentration polarizations at the membrane surface originating from zero-current transmembrane ion fluxes. It is assumed that interfacial ion-transfer processes are considerably faster than bulk diffusion processes, so that local interfacial equilibrium still exists. Consequently, the phase boundary potential, E_{PB}, is expected to still be valid in the presence of ion fluxes:

$$E_{PB} = \frac{RT}{z_I F} \ln \frac{k_I c_I}{[I^{z_I+}]} \quad (5)$$

where k_I is a function of the standard free energy of transfer for ion I and c_I and $[I^{z_I+}]$ are the boundary concentrations of I in the aqueous and organic phases, respectively.[12,26] Transmembrane ion fluxes, under zero-current conditions, induce concentration gradients of primary and interfering ions in the membrane and in the unstirred diffusion layer of the sample so that c_I and $[I^{z_I+}]$ are different from the respective concentrations in the bulk of the sample and in the inner phase boundary layer of the membrane. Theoretical models describing the response of ISEs in the presence of zero-current ion fluxes[15−17] calculate the ion activities in the phase boundary region of both phases at the sample side of the membrane as a function of the compositions of the bulk of the sample and of the membrane at its reference side. In previous treatments, the models were based on fundamental relationships, i.e., ion-exchange and coextraction equilibria at the sample−membrane interface and coupled steady-state co- and counter-diffusion fluxes in both phases.[15−17] By making use of the experimentally accessible selectivity coefficients instead of ion-exchange constants and single-ion distribution coefficients, this paper takes a more direct approach that is easier to apply and yields explicit solutions for many practically relevant cases. The

(19) Meier, P. C. *Anal. Chim. Acta* **1982**, *136*, 363.
(20) Hung, L. Q. *J. Electroanal. Chem.* **1983**, *149*, 1.
(21) Kakiuchi, T. *Anal. Chem.* **1996**, *68*, 3658.
(22) Bakker, E.; Nägele, M.; Schaller, U.; Pretsch, E. *Electroanalysis* **1995**, *7*, 817.
(23) Nägele, M.; Bakker, E.; Pretsch, E. *Anal. Chem.* **1999**, *71*, 1041.
(24) Bakker, E.; Meruva, R. K.; Pretsch, E.; Meyerhoff, M. E. *Anal. Chem.* **1994**, *66*, 3021.
(25) Guilbault, G. G.; Durst, R. A.; Frant, M. S.; Freiser, H.; Hansen, E. H.; Light, T. S.; Pungor, E.; Rechnitz, G.; Rice, N. M.; Rohm, T. J.; Simon, W.; Thomas, J. D. R. *Pure Appl. Chem.* **1976**, *48*, 127.
(26) Morf, W. E. *The Principles of Ion-Selective Electrodes and of Membrane Transport*; Elsevier: New York, 1981.

present model is based on our previously introduced formalism (eq 2) that predicts the emf as a function of the composition of the sample that may contain any number of interfering ions.[23] The phase boundary equilibrium and the condition of equal fluxes in both phases supply the equations necessary to calculate the unknown concentrations of the primary ion in the surface layer of both phases at the sample side of the membrane, which are then used to calculate the phase boundary potential (eq 5).

In the absence of interferences, the response function is described by the Nernst equation (eq 3). The term $k_I/[I^{z_I+}]$ of the phase boundary potential model (eq 5) is then constant and included in E_I^0 of eq 3. To describe the response function in the presence of interfering ions, a_I is replaced by the logarithmic term of eq 2. Another view of interferences is obtained from the phase boundary potential model (eq 5). An interfering cation increases the phase boundary potential because it reduces the concentration $[I^{z_I+}]$ by an ion-exchange process (cf. eq 5). In other words, a_I is not replaced by the corresponding term of eq 2, but it is kept at its constant value and the interference is described by a change of E_I^0 as a consequence of the decrease of $[I^{z_I+}]$. Since both views describe the same process, the decrease of $[I^{z_I+}]$ in eq 5 is equivalent to the increase of the logarithmic term (eqs 2 vs 3).

In the following, the primary ion in the membrane is assumed to be strongly complexed by an ionophore. It is assumed that the concentration of uncomplexed ionophore is constant; i.e., it is present in large excess relative to the ion-exchanger concentration. As a consequence, a change in concentration of primary ion complex is always proportional to a change in concentration of the free primary ion in the membrane. For a membrane without interference, the concentration of this complex (stoichiometry 1:n) is dictated by the concentration of lipophilic ion exchanger, R_T ($[IL_n^{z_I+}]_0 = R_T/z_I$). The membrane potential can therefore be rewritten on the basis of eq 5 as

$$E_M = E_I^0 + \frac{RT}{z_I F}\ln\frac{R_T}{z_I} + \frac{RT}{z_I F}\ln\frac{c_I}{[IL_n^{z_I+}]} \qquad (6)$$

Equations 2 and 6 describe the same process and are fully equivalent. They are now combined to give the important relationship between membrane selectivity and phase boundary concentrations:

$$\frac{c_I}{[IL_n^{z_I+}]} = \frac{z_I}{R_T}\left[\frac{1}{2}\sum_{m1} K_{I,m1}^{pot\ 1/z_I} c_{m1} + \sqrt{\left(\frac{1}{2}\sum_{m1} K_{I,m1}^{pot\ 1/z_I} c_{m1}\right)^2 + \sum_{m2} K_{I,m2}^{pot\ 2/z_I} c_{m2}}\right]^{z_I} \qquad (7)$$

The second relationship required for treating the response of low detection limit ion-selective electrodes is the steady-state flux equation.[15−17] The ratio of the concentration difference in diffusion layer of the sample to the concentration difference in the membrane is constant:

$$\frac{c_I - c_{I,bulk}}{[IL_n^{z_I+}]' - [IL_n^{z_I+}]} = q \qquad (8)$$

where c_I and $c_{I,bulk}$ are the concentrations of I^{z_I+} at the phase boundary and in the sample bulk and $[IL_n^{z_I+}]'$ and $[IL_n^{z_I+}]$ are the concentrations of primary ion complex at the inner and outer sides of the membrane. The value q is given by

$$q = D_{org}\delta_{aq}/D_{aq}\delta_{org} \qquad (9)$$

where D and δ are the diffusion coefficients and the Nernst diffusion layer thicknesses in the indicated phases. The two unknowns $[IL_n^{z_I+}]$ and c_I are obtained from the two eqs 7 and 8 for any number of interfering ions, as a function of the concentration of complex at the inner membrane side and for a given sample composition. It is realistically assumed here that the interfering ions are more concentrated than the primary ion, and therefore their concentration polarization in the diffusion layer of the sample can be neglected. Explicit solutions for the case of primary and interfering ions having the same charge are shown here. Other charge combinations are treated in the Supporting Information.

For ions of the same charge, eq 2 is significantly simplified to the established Nicolsky−Eisenman equation (eq 1). This can be combined with eqs 7 and 8 to eliminate the concentration of primary ion complex in the membrane phase boundary contacting the sample. Solving for the boundary concentration of the primary ion c_I, yields the following explicit equation:

$$c_I = \frac{1}{2}\left(c_{I,bulk} - \sum K_{IJ}^{pot} c_J + [IL_n^{z_I+}]'q - \frac{qR_T}{z_I} + \left(\left(c_{I,bulk} - \sum K_{IJ}^{pot} c_J + [IL_n^{z_I+}]'q - \frac{qR_T}{z_I}\right)^2 + 4\sum K_{IJ}^{pot} c_J\,([IL_n^{z_I+}]'q + c_{I,bulk})\right)^{1/2}\right) \qquad (10)$$

Equation 10 quantifies how the phase boundary concentration changes for any given bulk sample composition, $c_{I,bulk}$, and fixed inner concentration $[IL_n^{z_I+}]'$ of the primary ion complex. This inner concentration can be kept constant by utilizing an appropriate ion buffered inner solution. The actual response function is obtained by inserting eq 10 into the Nicolsky−Eisenman equation (eq 1) to yield

$$E = E_I^0 + \frac{RT}{z_I F}\ln\left(\frac{1}{2}\left(c_{I,bulk} + \sum K_{IJ}^{pot} c_J + [IL_n^{z_I+}]'q - \frac{qR_T}{z_I}\right) + \frac{1}{2}\left(\left(c_{I,bulk} - \sum K_{IJ}^{pot} c_J + [IL_n^{z_I+}]'q - \frac{qR_T}{z_I}\right)^2 + 4\sum K_{IJ}^{pot} c_J\,([IL_n^{z_I+}]'q + c_{I,bulk})\right)^{1/2}\right) \qquad (11)$$

Equation 11 is a general extension of the Nicolsky−Eisenman eq 1, by taking into account steady-state zero-current transmembrane ion fluxes. It is equivalent to eq 23 given in ref 17.

If the effects of coextraction at the inner membrane side are either insignificant or are perfectly counterbalanced by ion exchange, the fixed inner concentration $[IL_n^{z_I+}]'$ is given by the amount of lipophilic ion exchanger in the membrane ($[IL_n^{z_I+}]' = R_T/z_I$). This leads to an ion response curve with a Nernstian slope, described by simplifying eq 11:

$$E = E_I^0 + \frac{RT}{z_I F} \ln\left(\frac{1}{2}(c_{I,bulk} + \sum K_{IJ}^{pot} c_J) + \frac{1}{2}\left((c_{I,bulk} - \sum K_{IJ}^{pot} c_J)^2 + 4 \sum K_{IJ}^{pot} c_J \left(q\frac{R_T}{z_I} + c_{I,bulk}\right)\right)^{1/2}\right) \quad (12)$$

At the detection limit ($c_{I,bulk} = 0$), eq 12 further simplifies to

$$E = E_I^0 + \frac{RT}{z_I F} \ln\left(\frac{1}{2} \sum K_{IJ}^{pot} c_J + \frac{1}{2}\left((\sum K_{IJ}^{pot} c_J)^2 + \frac{qR_T}{z_I} 4 \sum K_{IJ}^{pot} c_J\right)^{1/2}\right) \quad (13)$$

and the logarithmic detection limit is described by the log term of eq 13:

$$\log c_I(DL) = \log\left(\frac{1}{2} \sum K_{IJ}^{pot} c_J + \frac{1}{2}\left((\sum K_{IJ}^{pot} c_J)^2 + \frac{qR_T}{z_I} 4 \sum K_{IJ}^{pot} c_J\right)^{1/2}\right) \quad (14)$$

If ion fluxes are not relevant ($4qR_T/z_I \ll K_{IJ}^{pot} c_J$), eq 13 readily reduces to the traditional eq 4. On the other hand, if $4qR_T/z_I \gg K_{IJ}^{pot} c_J$, i.e., for highly selective electrodes, eq 14 is simplified to the following relationship:

$$\log c_I(DL) = \frac{1}{2} \log\left(\frac{qR_T}{z_I} \sum K_{IJ}^{pot} c_J\right) \quad (15)$$

Since $4qR_T/z_I$ is typically on the order of 10^{-6} M,[11] eq 15 will already be valid for a number of situations where the interfering ion concentration is low or the electrode exhibits a fair to good selectivity over the interfering ions.

Equation 15, and eqs 30 and 39 from the Supporting Information for other charge combinations, can be conveniently combined into one universal relationship:

$$\log c_I(DL) = \left(\frac{1}{2} + (z_J - z_I)\frac{1}{6}\right) \log\left(\left(\frac{qR_T}{z_I}\right)^{z_I/z_J} \sum K_{IJ}^{pot} c_J^{z_I/z_J}\right) \quad (16)$$

This equation should be valid for primary and interfering ions that have an equal charge or that are divalent/monovalent or monovalent/divalent. As stated above, eq 16 also assumes that ion-exchange and coextraction processes are either insignificant or counterbalanced at the inner membrane side.

Further Improvement of the Detection Limit: ISEs with Apparent Super-Nernstian Response. Equation 16 describes the optimum detection limit if a Nernstian slope is observed throughout most of the calibration curve. It has been shown, however, that the detection limit may be further improved if a small negative deviation of the potential from the Nernstian response curve is allowed. This is achieved by utilizing an inner electrolyte composition that induces a small inward ion flux, with $[IL_n^{z_I+}]'$ being smaller than R_T/z_I. According to the recently introduced definition of the lower detection limit, a deviation of the emf by $R_T/z_I F \ln 2$ from the extrapolated linear Nernstian segment of the calibration curve is tolerable.[15] For a monovalent primary ion such as Ag^+, this value is 17.8 mV at 25 C. It corresponds to an allowed sample depletion at which the surface concentration is half the bulk sample concentration ($c_I = c_{I,bulk}/2$). Based on these recommendations, modified equations for the detection limit are developed here for comparison purposes. As above, a more detailed derivation will first be given for primary and interfering ions of the same charge, followed by the end results for the other two cases.

The optimal concentration $[IL_n^{z_I+}]'$ to obtain this tolerable super-Nernstian response range is found by inserting the relationship $c_I = c_{I,bulk}/2$ into eq 10:

$$[IL_n^{z_I+}]' = -\frac{z_I c_{I,bulk}^2 - 2qR_T c_{I,bulk} + 2z_I c_{I,bulk} \sum K_{IJ}^{pot} c_J}{2z_I(c_{I,bulk} q + 2q \sum K_{IJ}^{pot} c_J)} \quad (17)$$

This limiting inner concentration of the complex is different for every sample composition. The largest value for the entire calibration curve is found by setting the derivative of eq 17 with respective to $c_{I,bulk}$ equal to zero. The result is solved for this critical bulk sample concentration $c_{I,bulk}$(max depletion) to give

$$c_{I,bulk}(\text{max depletion}) = 2\sqrt{\frac{qR_T}{z_I} \sum K_{IJ}^{pot} c_J} - 2\sum K_{IJ}^{pot} c_J \quad (18)$$

It describes the bulk primary ion concentration at which maximum depletion occurs. This relationship is inserted back into eq 17 to give the optimum concentration of primary ion complexes at the inner membrane side:

$$[IL_n^{z_I+}]' = \left(\sqrt{\frac{R_T}{z_I}} - \sqrt{\frac{1}{q} \sum K_{IJ}^{pot} c_J}\right)^2 \quad (19)$$

This surprisingly simple equation is very useful in predicting appropriate inner electrolyte compositions, by utilizing ion buffers and calculating the resulting concentration of primary ion complex at the inner side of the membrane with eq 7 (c_I and $c_{I,bulk}$ are assumed to be identical in the ion buffered inner solutions). Note that eq 19 is formulated on the basis of sample interference; i.e., the noted concentrations of interference are those of the sample. Consequently, the optimal inner solution composition is predicted by combining eq 19 and the simplified eq 7 (for the inner solution, with a primary ion concentration c_I' and interfering ions c_K') to give

$$c_I' = \frac{z_I}{R_T}[c_I' + \sum_K K_{IK}^{pot} c_K'] \left(\sqrt{\frac{R_T}{z_I}} - \sqrt{\frac{1}{q} \sum_J K_{IJ}^{pot} c_J}\right)^2 \quad (20)$$

This simple equation shows the optimal relationship between inner solution concentrations (c_I' and any interfering ions c_K') as a

function of the sample composition (c_J). Finally, the optimal response curve, by allowing a small super-Nernstian response slope, is given by inserting eq 19 into eq 11:

$$E = E_I^0 + \frac{RT}{z_I F}\ln\left(\frac{c_{I,bulk}}{2} - \left(\frac{qR_T}{z_I}\sum K_{IJ}^{pot} c_J\right)^{1/2} + \frac{1}{2}\left(\frac{8qR_T}{z_I}\sum K_{IJ}^{pot} c_J + \left(\frac{c_{I,bulk}}{2} + \frac{1}{z_I}\sum K_{IJ}^{pot} c_J\right)^2 - \left(\frac{qR_T}{z_I}\sum K_{IJ}^{pot} c_J (c_{I,bulk} + 2\sum K_{IJ}^{pot} c_J)\right)^{1/2}\right)^{1/2}\right) \quad (21)$$

This explicit formula assumes that the detection limit is fully dictated by a counterdiffusion flux owing to an ion-exchange reaction at the sample−membrane interface that cannot fully be compensated for at the internal side of the membrane. In dilute solutions where the extent of ion exchange is small, eq 21 can be simplified to calculate the expected optimal detection limit as

$$\log c_I(DL) = \frac{1}{2}\log\left(\frac{qR_T}{z_I}\sum K_{IJ}^{pot} c_J\right) + \log(\sqrt{2} - 1) \quad (22)$$

The second log term that corresponds to the improvement from accepting a small deviation from Nernstian response is equal to −0.38. This is accomplished by exchanging a small fraction of primary ions with another ion at the inner membrane side. Otherwise, the equation is identical to eq 15, where no super-Nernstian response slope was allowed. Note that an analogous treatment for more complex charge combinations is presented in the Supporting Information.

RESULTS AND DISCUSSION

According to the traditional definition of the detection limit (eq 4), a monovalent ion-selective electrode with a selectivity coefficient of $\log K_{I,Li}^{pot} = -7.7$, for example, is expected to show a detection limit of $a_I = 10^{-12.7}$ M in the presence of a background of 10^{-5} M $LiNO_3$. Such a low detection limit cannot be observed at present because of zero-current concentration polarizations originating from transmembrane counterdiffusion ion fluxes. The theoretical model treats such processes adequately for the steady state. It is simplified and more practical relative to earlier works[15−17] because it describes the concentration of the primary ion in the membrane phase boundary on the basis of the directly accessible selectivity coefficients of the membrane.

The expected ISE response curves for two different Ag^+-selective electrodes, again with $\log K_{Ag,Li}^{pot} = -7.7$ and 10^{-5} M Li^+ as the main interference are shown in Figures 1 and 2. The response in Figure 1 is calculated according to eq 12 by assuming that the concentration of the primary ion complex at the inner side of the membrane exactly matches that of the lipophilic ion exchanger. This means that coextraction effects must be either insignificant or perfectly compensated by ion exchange, which is accomplished with an appropriate inner solution composition. It is further assumed that the concentration of ion exchanger in the membrane is 5.7 mM and that the kinetic factor q (see eq 9) is 10^{-3} (see ref 11). Although the expected detection limit with $\log c_I(DL) = -9.0$ is respectable, it is much higher than the value

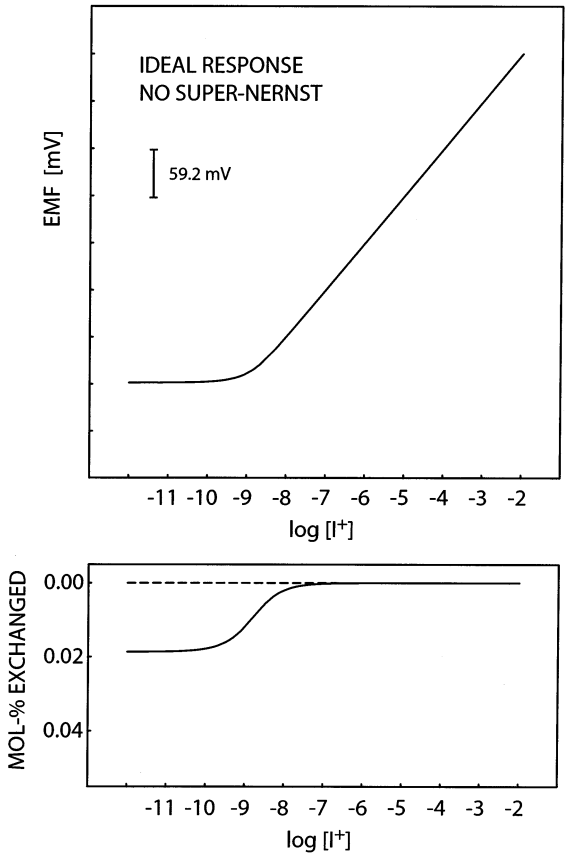

Figure 1. Top: theoretical response curve according to eq 12, for an ISE where ion-exchange and coextraction processes are perfectly compensated for at the inner membrane side ($[IL_n^{z_I+}]' = R_T$). This represents the lowest possible detection limit without observing any super-Nernstian response slope. Parameters used were $R_T = 0.0057$ mol kg^{-1}, $q = 10^{-3}$, and $\log \sum K_{IJ}^{pot} c_J = -12.7$. Bottom: percent of ionophore complex concentration at the membrane side facing the inner electrolyte (dotted line) and the sample (solid line). The outer concentration is obtained by inserting the result of eq 10 into eq 7 and solving for $[IL_n^{z_I+}]$. A very small (0.02%) exchange of primary ion complex by another sample ion already induces a sufficiently large transmembrane flux to reach the detection limit.

−12.7 anticipated on the basis of eq 4. The relative concentration of primary ion complex, at the sample side of the membrane and at steady state, is shown in the bottom part of Figure 1 for the entire response curve (obtained by inserting c_I from eq 10 into eq 7 and solving for $[IL_n^{z_I+}]$). The dotted line at 100% indicates the concentration of complex at the inner membrane side, $[IL_n^{z_I+}]'$, which remains unchanged for the entire concentration range. Even at a relatively high sample concentration, a slight ion exchange with Li^+ at the sample side is evident, although it has no effect on the observed potential. At the lowest bulk silver concentrations, on the other hand, the mere 0.02% of the Ag^+ complex that has been displaced by Li^+ at the sample side is sufficient to make the electrode completely nonresponsive to bulk Ag^+ concentrations. A sigmoidal change of the primary ion complex concentration at the phase boundary is obtained for Ag^+ concentrations around the detection limit. This figure illustrates convincingly that it is very difficult to quantitatively exchange primary ions from the membrane with an interfering ion that is significantly discriminated. Even at bulk sample activities that are far below the detection limit, Ag^+ remains the potential determining ion because

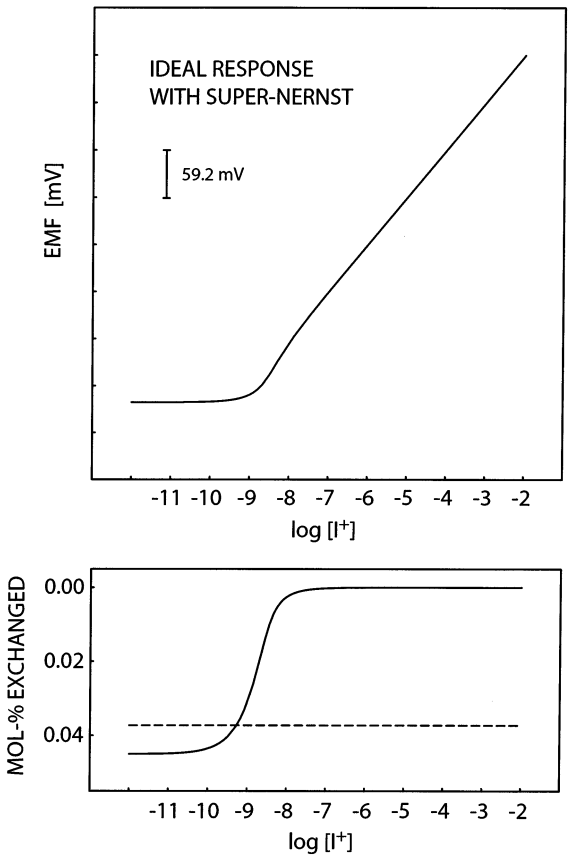

Figure 2. Top: theoretical response curve according to eq 11, for an ISE where an optimal ion-exchange process is induced at the inner membrane side (see eq 19). This represents the lowest possible detection limit by observing a small, tolerable super-Nernstian response slope. Parameters used were as in Figure 1. Bottom: percent of ionophore complex concentration at inner (dotted line) and outer (solid line) membrane side. The outer concentration is obtained as in Figure 1, while the inner concentration was determined with eq 19.

of this leaching process from the membrane.[27] The response curve shown in Figure 1 would show a drastically worsened detection limit for $[IL_n^{z_I+}]'$ that is even just slightly larger than R_T/z_I, as recently established.[28] It also clearly illustrates why routine selectivity determinations, with methods recommended by IUPAC,[25] must yield apparent selectivities that are much worse than the true values. Consequently, it has been recently recommended that the Nernstian response slopes must be experimentally confirmed for each separately evaluated interfering ion.[13]

Figure 2 shows the predicted response curve for the same membrane as in Figure 1, but with an internal filling solution that gives a slightly reduced concentration of Ag^+ complex at the inner side of the membrane. The Ag^+ concentration at the inner side is chosen so that the curve would deviate exactly 17.8 mV from the Nernstian response curve, which corresponds to the maximum tolerable value for a monovalent ion-selective electrode.[15] This optimal reduced concentration can, for the first time, be conveniently calculated with eq 19, while the entire ISE response curve is explicitly described with eq 21. The silver ion concentration at the inner side is reduced by just 0.04%, which induces a counterdiffusion flux of silver ions toward the inner solution. According to the theory developed above (see eq 22), the detection limit can be decreased by roughly another half order of magnitude compared to the curve shown in Figure 1. As in Figure 1, the constant concentration of silver ion complex at the inner side is indicated as a dotted line on the bottom part of the curve. The concentration of silver ion complex at the sample side, $[IL_n^{z_I+}]$, calculated by inserting eq 19 into eq 7, is shown as a solid line on the bottom plot. Again, the concentration of the Ag^+ complex starts to decrease as less silver is present in the sample. Because some silver is already exchanged at the inner membrane side, at very low sample concentrations, the extent of ion exchange at the sample side is somewhat larger than in the case shown in Figure 1. The cross section of the solid and dotted lines corresponds to the situation where no primary ion gradient exists across the membrane at steady state. A sufficient portion of Ag^+ is replaced by Li^+ at the sample side of the membrane so that it now perfectly matches the concentration at the inner side. While the sample concentration is very close to the detection limit, neither sample depletion nor primary ion release from the membrane take place here, so that this point lies perfectly on the Nernstian response curve. The fact that the solid line dips under the dotted line upon further sample dilution indicates a reversal of the direction of the silver ion flux. As in Figure 1, the detection limit is now again fully dictated by silver ions leaching from the membrane into the sample. The smaller concentration gradient in the membrane in comparison with Figure 1 indicates that this ISE reaches a lower detection limit (see eq 8).

The response curves shown in Figures 1 and 2 were cacluated for a selected ISE with characteristics that are close to the presented experimental cases (see below). They indicate that in the presence of ion fluxes the lower detection limit is by 3−4 orders of magnitude higher than expected according to the traditional models. However, as eq 16 shows for various charge combinations of primary and interfering ions, the traditional model is valid in limiting cases; for example, when selectivities are poor, ion fluxes through the membrane are slow (q small) or the concentration of the interfering ion is high. The theory developed above is now used to predict the lower detection limits as a function of selectivity coefficients log $K_{I,J}^{pot}$ at two concentrations of the interfering ion J for various combinations of z_I and z_J. The results of the calculations are presented in Figure 3. At $c_J = 0.1$ M, and poor selectivities (right-hand side of the top curves), the lower detection limit linearly decreases with decreasing selectivity coefficients according to the classical eq 4. The curves are shifted relative to one another because of the power term (z_I/z_J) of eq 4. However, when not the traditional interference but rather the ion release induced by very small ion exchange determines the lower detection limit (left side), the curves are flatter; i.e., a larger decrease of the selectivity coefficients is required to improve the detection limit. The effect is most extreme for divalent primary ions with monovalent interfering ions. The plots on the bottom of Figure 3 indicate that, at low concentrations of interfering ions (0.1 mM), the traditional model only applies for membranes with very poor selectivities. For the most extreme case, i.e., $z_I = 2$ and $z_J = 1$, it is not applicable at all. It must be noted that the determination of selectivity coefficients according to the fixed interference or separate solution methods would give erroneous

(27) Bakker, E. *Anal. Chem.* **1997**, *69*, 1061.
(28) Mathison, S.; Bakker, E. *Anal. Chem.* **1998**, *70*, 303.

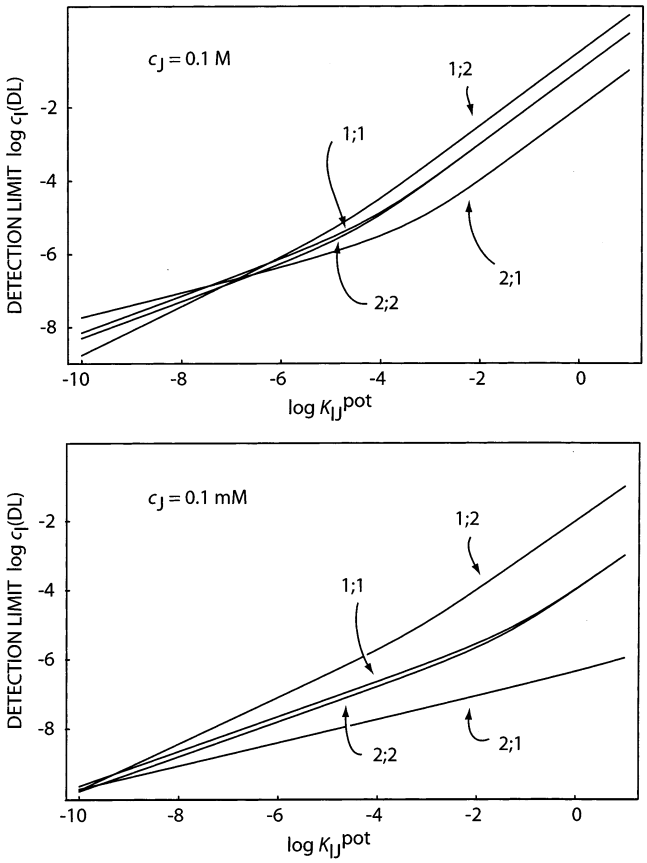

Figure 3. Calculated logarithmic detection limit for an optimal ISE as a function of selectivity coefficient, shown for a 0.1 M (top) and 0.1 mM (bottom) sample background ion and for the indicated charges of the primary (first number) and interfering ion (number after semicolon). As in Figure 1, no coextraction or ion-exchange processes are assumed to take place at the inner membrane side. The curves are calculated with eqs 14, 29, and 38 (see Supplementary Information for the last two equations), by utilizing the same q and R_T as for Figure 1. Detection limit predictions approach eq 4 at higher concentrations and eq 16 at lower concentrations.

results in all cases where the traditional model is not applicable. In principle, the bias could be detected by evaluating the response slope toward the interfering ion,[29] but traditionally this has not been done.[13] It is also apparent from the curves in Figure 3 that, for low detection limits in the presence of a relative high concentration of interfering ions, i.e., for trace level analysis, the traditional model cannot be applied. On the other hand, it must be kept in mind that the ultimate lower detection limits are given by the traditional model. They may eventually be reached if ion flux effects can be eliminated by altering the experimental setup.

Equation 16 is now used to predict the required selectivity coefficients for the most important interfering ions in order to obtain 10^{-7} and 10^{-9} M detection limits of any monovalent or divalent heavy metal ion in environmental sweet water samples.[30] As follows from the above discussion, these selectivities must be much better than estimated by the established equations that neglect ion fluxes. Table 1 shows that rather high selectivities are required, especially in order to reach nanomolar detection limits. On the other hand, it must be realized that, based on recent results,[5,27] such good selectivities are not uncommon. Only the traditionally determined highly biased selectivity values suggested a much worsened selectivity behavior.

The theoretical approach described above allows one to predict the optimal composition of the inner solution of a Ag^+-selective electrode (see eq 19, which is for primary and interfering ions of the same charge). Evidently, the optimal composition depends on the typical background electrolyte of the target sample, because even the presence of highly discriminated interfering ions may induce the exchange of some minor amounts of primary ions by interfering ones in the membrane. It also depends on the concentration of the ion exchanger in the membrane and the kinetic factor q (see eq 9). As shown by Figure 1, the exchange of less than 0.1% of the primary ion at the sample side may already be highly relevant. The optimal inner solution will compensate for this effect by the exchange of a similar portion of the primary ion in the inner membrane surface layer.

First, the selectivity coefficients of the membrane had to be determined. The response slope must be checked with each separately determined interfering ion because it is essential that the experimental selectivity coefficients are unbiased.[13] The selectivity coefficients can be used to calculate the composition of the membrane surface layer in contact with a given aqueous solution (see eq 7). Their knowledge allows one to predict the full response curves in the presence of relevant ion fluxes (eq 11).

Initial work of fabricating a Ag^+-selective electrode with a low detection limit focused on the well-established ionophore methylene bis(diisobutyldithiocarbamate) (MBDiBDTC).[31] The selectivity of the resulting membranes was excellent, and detection limits were reached that were, with 10 ppt (10^{-10} M), perfectly in line with the theoretical expectations outlined above (data not shown). Unfortunately, however, these results were poorly reproducible and the electrodes also showed strong potential drifts at high concentrations, even after much experimentation. It is possible that this ionophore interacts too strongly with silver ions and undergoes chemical decomposition. It was therefore decided to explore a potentially more robust ionophore that is based on thioether, rather than dithiocarbamate functionalities. The ionophore *O,O″*-bis[2-(methylthio)ethyl]-*tert*-butylcalix[4]arene[32,33] proved to be an adequate choice, although the selectivity of this ionophore over alkali metals is known to be somewhat poorer than the previously mentioned ionophore. Unbiased selectivity coefficients were obtained as log $K_{Ag,Li}^{pot} = -7.7 \pm 0.2$, log $K_{Ag,Na}^{pot} = -7.4 \pm 0.2$, log $K_{Ag,K}^{pot} = -6.6 \pm 0.1$, and log $K_{Ag,H}^{pot} = -6.8 \pm 0.2$. The slope toward Ag^+ was found to be Nernstian, and the slopes toward the interferences were between 52 and 58 mV decade^{-1}. The selectivities are much better[27,34] than originally obtained with traditional methods.[32,33]

As a next step, the inner solution was optimized to give the best ionophore complex concentration at the inner membrane side. According to theory, this optimal concentration must be in the range between the value calculated with eq 19 and the total

(29) Ceresa, A.; Pretsch, E. *Anal. Chim. Acta* **1999**, *395*, 41.
(30) Sigg, L.; Stumm, W. *Aquatische Chemie*; B. G. Teubner: Stuttgart, 1994.
(31) Kamata, S.; Onoyama, K. *Anal. Chem.* **1991**, *63*, 1295.
(32) Cobben, P. L. H. M.; Egberink, R. J. M.; Bomer, J. B.; Bergveld, P.; Verboom, W.; Reinhoudt, D. N. *J. Am. Chem. Soc.* **1992**, *114*, 10573.
(33) Malinowska, E.; Brzózka, Z.; Kasiura, K.; Egberink, R. J. M.; Reinhoudt, D. N. *Anal. Chim. Acta* **1994**, *298*, 245.
(34) Bakker, E. *Sens. Actuators, B* **1996**, *35*, 20.

Table 1. Required Selectivity Coefficients To Achieve 10^{-7} and 10^{-9} M Detection Limit in Sweet Water Samples[a]

	logarithmic molar concentrations of interference[b]							
	H^+		Na^+		Mg^{2+}		Ca^{2+}	
	low	high	low	high	low	high	low	high
	−8.5	−4.0	−4.6	−2.6	−4.8	−2.8	−4.3	−2.5
	For 10^{-7} M Detection Limit							
required log K_{IJ}^{pot} ($z_I = 1$)	0.8	−3.7	−3.1	−5.1	−4.9	−5.9	−5.2	−6.1
required log K_{IJ}^{pot} ($z_I = 2$)	9.2	0.2	1.4	−2.6	−2.6	−4.6	−3.1	−4.9
	For 10^{-9} M Detection Limit							
required log K_{IJ}^{pot} ($z_I = 1$)	−3.2	−7.7	−7.1	−9.1	−7.9	−8.9	−8.2	−9.1
required log K_{IJ}^{pot} ($z_I = 2$)	3.2	−5.8	−4.6	−8.6	−6.6	−8.6	−7.1	−8.9

[a] According to eq 16, with $R_T = 0.5$ mmol kg^{-1} and $q = 0.001$. [b] Indicated low and high concentration boundaries are according to ref 30.

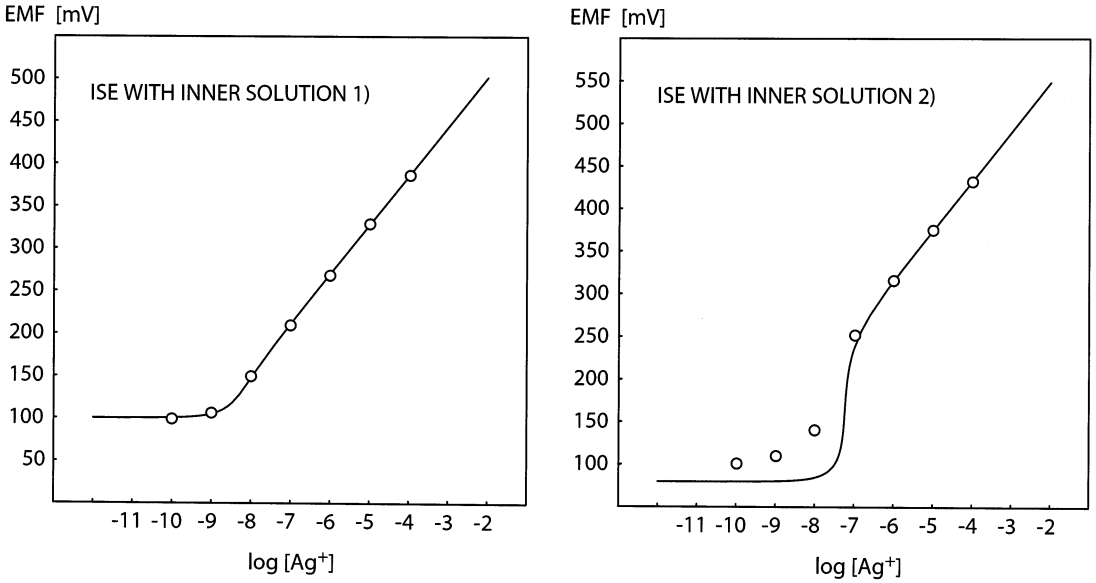

Figure 4. Left: experimental response function to silver ions for a silver-selective ISE whose inner solution composition was optimized to give an optimal low detection limit. The theoretical response curve according to eq 11 with $[IL_n^{z_i^+}]' = 0.005\ 697$ mol kg^{-1} is shown as a solid line (see text). Right: corresponding response function for an identical ISE, but whose inner solution composition was chosen to exchange a larger portion (1%) of silver ions from the inner membrane side. The theoretical response curve according to eq 11 with $[IL_n^{z_i^+}]' = 0.005\ 643$ mol kg^{-1} is shown as a solid line (see text).

ion-exchanger concentration R_T (0.0057 mol kg^{-1}). Owing to the very small, yet undetermined influence of coextraction of the silver salt into the inner side of the membrane, eq 19 was used to calculate the desired value. The target sample concentration was chosen as 10^{-5} M $LiNO_3$ at pH 5.4. The two interferences, Li^+ and H^+, can be combined into one $K_{IJ}^{pot}c_J$ term, 8.3×10^{-13}, because the ions have the same charge. This value was inserted into eq 19, with $q = 0.001$ and $R_T = 0.0057$ mol kg^{-1}, to yield the desired concentration of the silver complex at the membrane inner side as 0.005 679 mol kg^{-1}. For a justification of the value of q, see ref 11. The result corresponds to a 0.05% exchange of silver ions by another ion at the inner membrane side and is somewhat larger than the value shown in Figure 2, bottom, where the interference by H^+ ions was not considered. In earlier work, the composition of the inner solution was optimized for low detection limit applications by keeping a sufficiently high activity of an interfering ion and a controlled low activity of the primary ion. The latter has most often been adjusted with ion buffers such as EDTA or NTA. It seems, however, that even the complexes of these highly hydrophilic complexing agents may partition into the organic membrane phase to some extent.[35] Such additional partitioning processes would complicate the experimental planning of inner filling solutions by calculation. Therefore, an ion-exchange resin was used here to maintain a constant low concentration of the primary ion (see Experimental Section). The resin is not expected to partition into the organic phase. Equation 20 shows that the desired concentration of silver in the inner filling solution can be calculated as $c_{Ag}' = 3.2 \times 10^{-7}$ M if the sodium concentration is $c_{Na}' = 4 \times 10^{-3}$ M (log $K_{Ag,Na}^{pot} = -7.4$) and the sample contains the selectivity-weighted concentration of interfering ions $\sum K_{IJ}^{pot}c_J = 8.3 \times 10^{-13}$ M. As explained in the Experimental Section, such a composition was achieved by equilibrating the sodium form of the resin with the desired total amount of silver salt in water.

The calibration curve of the resulting ISE A in 10^{-5} M $LiNO_3$ is presented in Figure 4, left. The experimental data match the

(35) Ion, A. C.; Bakker, E.; Pretsch, E. *Anal. Chim. Acta* **2001**, *440*, 71.

theoretical predictions very nicely, which were obtained with eq 11 by using $R_T = 0.0057$ mol kg^{-1}, $q = 10^{-3}$, $\sum K_{IJ}^{pot} c_J = 8.3 \times 10^{-13}$ M, and $[IL_n^{z_I+}]' = 0.005\,697$ mol kg^{-1}. The observed detection limit was $\sim 10^{-9}$ M (100 ppt) Ag^+, with a standard deviation for the log(detection limit) of 0.08. This value is not the ultimate low limit for the potentiometric detection of silver ions, but it represents the lowest expected detection limit for the chosen membrane and sample composition. Another inner filling solution composition was also explored that would yield an apparently super-Nernstian response slope. In this case, the inner filling solution B was chosen with $c_{Ag} = 8.3 \times 10^{-9}$ M and $c_{Na} = 2.1 \times 10^{-3}$ M, which would exchange just about 1% of silver ions at the inner membrane side ($[IL_n^{z_I+}]' = 0.005\,643$ mol kg^{-1} in eq 10). The corresponding electrode response function is shown in Figure 4, right, together with the theoretical curve on the basis of eq 10 and by using the same parameters as in Figure 4, left, but with the different $[IL_n^{z_I+}]'$ value. Evidently, the theoretical curve describes the experimental data very well but predicts a steeper potential drop below 10^{-7} M than experimentally observed. Indeed, the experimental data for the concentrations below the potential drop still showed a potential drift of up to -3 mV h^{-1} when recorded. This suggests that the concentration profiles across the membrane at the lowest concentrations were not yet perfectly at steady state, which is what the theory would expect. Nonetheless, the predictions are a very good match with the data, and this marks the first time where such a close correlation was attempted and also observed.

CONCLUSIONS

The simplified steady-state model equations introduced in this paper make it possible to apply a much more rational design of ISEs for trace level measurements. Once the thermodynamic selectivities of a membrane are determined experimentally, the optimal composition of the inner solution can be predicted for any target sample. For inner solutions that contain ion-exchange resins, the experiments quantitatively follow the theoretical predictions. Correspondence is also very good for the case where the ISE shows a super-Nernstian response slope region, because too many primary ions were exchanged at the inner membrane side. Theory also offers insights into the expected detection limit improvement by allowing a small super-Nernstian response slope, which is almost half an order of magnitude. Unlike earlier treatments, an explicit, rather simple equation can now be used for ions of the same charge to describe the response function of an ISE with any given inner electrolyte composition, as long as this composition remains constant. It is anticipated that the development of potentiometric low detection limit ISEs will be significantly facilitated with the help of the theoretical tools presented here.

ACKNOWLEDGMENT

This work was financially supported by the National Institutes of Health (Grant R01-GM59716), The Swiss National Science Foundation, and Orion Research Inc. (Beverly, MA).

SUPPORTING INFORMATION AVAILABLE

Additional information as noted in the text. This material is available free of charge via the Internet at http://pubs.acs.org.

Received for review January 28, 2002. Accepted May 24, 2002.

AC025548Y